

1 **Solvent-controlled formation of monomeric and dimeric species containing Cu(II) acetate and 4-**
2 **phenylpyridine**

3
4
5 Joan Soldevila-Sanmartín ^a, José A. Ayllón ^a, Teresa Calvet ^b, Mercè Font-Bardia ^c, Josefina Pons ^{a,*}
6
7
8
9
10
11
12
13
14
15
16

17 a Departament de Química, Universitat Autònoma de Barcelona, 08193 Bellaterra, Barcelona, Spain

18 b Cristal·lografia, Mineralogia i Dipòsits Minerals, Universitat de Barcelona, Martí i Franquès s/n,
19 08028 Barcelona, Spain

20 c Unitat de Difracció de Raig-X, Centres Científics i Tecnològics de la Universitat de Barcelona
21 (CCiTUB), Universitat de Barcelona, Solé i Sabarís, 1-3, 08028 Barcelona, Spain

22 .
23
24
25
26
27
28
29 Corresponding author at: Departament de Química, Universitat Autònoma de Barcelona, 08193-
30 Bellaterra-Cerdanyola, Barcelona, Spain. Fax: +34 93 581 31 01.

31 E-mail address: Josefina.Pons@uab.cat (J. Pons).
32

33 **ABSTRACT:**

34

35 Three copper(II) acetate complexes with 4-phenylpyridine (4-Phpy), namely [Cu(MeCO₂)₂(4-
36 Phpy)₂(H₂O)₂] (1), [Cu(MeCO₂)₂(4-Phpy)₂(H₂O)_{1.5}] (2) and [Cu(MeCO₂)₂(4-Phpy)]₂ (3), were
37 synthesized and characterized by analytical and spectroscopic methods. Experimental conditions as
38 solvent or temperature determine the species obtained. Crystal and molecular structure of 2 was
39 determined by X-ray diffraction. Compound 2 presents a singular structure, containing two
40 crystallographic independent mononuclear units [Cu(MeCO₂)₂(4-Phpy)₂(H₂O)₂] (2A) and
41 [Cu(MeCO₂)₂(4-Phpy)₂(H₂O)] (2B) in its unit cell and each of these forms an independent 1-D chain
42 through H-bonding.

43

44

45

46 1. INTRODUCTION

47

48 The formation of secondary building units (SBUs) with interesting supramolecular features in a
49 controlled fashion, such as 1D chains, 2D sheets or 3D porous frameworks is a current milestone in
50 inorganic chemistry [1–3]. In this topic, the combination of metal centers with carboxylates and
51 pyridines has attracted attention due the fact that pyridines provide structural rigidity and could force the
52 direction of the hydrogen bond propagation [4]. Cu(II) is a typical choice for metal center due its variety
53 of coordination modes and molecular topologies. An important family of Cu (II) based SBUs are
54 dimeric paddle-wheel like complexes [5,6]. Interestingly, when paddle-wheel like dimers crystallize,
55 usually mononuclear species with octahedral, square pyramidal or square planar geometries are also
56 formed. This dimer-monomer equilibrium in Cu(II) carboxylate derivatives with pyridines or other
57 auxiliary ligands has been known since decades and thoroughly studied [7–10]. Despite their efforts,
58 most studies do not provide a clear explanation of the mechanism that governs the formation of either
59 the dimeric or the monomeric compound. Furthermore, reports in the literature where the monomeric
60 and dimeric structures for the same choice ligands are isolated and characterized are scarce [11–13].
61 Recently in our group, we have assayed the reaction between $M(\text{MeCO}_2)_2 \cdot \text{H}_2\text{O}$ ($M = \text{Cu(II)}, \text{Zn(II)}$
62 or Cd(II) ; $\text{MeCO}_2 = \text{acetate}$), 1,3- benzodioxole-5-carboxylic acid (HPip) and different bulky pyridine
63 derivatives. Thus, dimeric and monomeric compounds were obtained [14–16]. Specifically, we have
64 assayed the reaction of $\text{Cu}(\text{MeCO}_2)_2 \cdot \text{H}_2\text{O}$, with HPip and 3-phenylpyridine (3-Phpy) or 4-
65 benzylpyridine (4-Bzpy), obtaining paddle-wheel dimers and mononuclear compounds in the same
66 reaction. However using 4-phenylpyridine (4-Phpy) only a dimeric compound $[\text{Cu}(\text{m-Pip})(\text{Pip})(4\text{-}$
67 $\text{Phpy})_2]$ is obtained [16].

68 As a continuation of these works, in this paper we study the reaction between $[\text{Cu}(\text{MeCO}_2)_2(\text{H}_2\text{O})]_2$
69 and 4-Phpy, a system that yields two new monomeric hydrated complexes besides the known paddle-
70 wheel dimeric compound [17]. All reactions were assayed at room temperature, and the obtaining of one
71 or another compound depends on the solvent employed in the preparations. All compounds were fully
72 characterized and the X-ray crystal structure of 2 is presented.

73 .

74 2. RESULTS AND DISCUSSION

75

76 2.1. Synthesis and general characterization

77 The reaction between $\text{Cu}(\text{MeCO}_2)_2 \cdot \text{H}_2\text{O}$ and 4-Phpy in a methanol: water (MeOH:H₂O, 1:1) mixture
78 as solvent at room temperature, using 1:1 Cu:4-Phpy molar ratio, yielded compound $[\text{Cu}(\text{MeCO}_2)_2(4\text{-Phpy})_2(\text{H}_2\text{O})_2]$ (1). However, the same reaction assayed in an ethanol:water (EtOH:H₂O, 1:1) mixture
79 as solvent results in the formation of compound $[\text{Cu}(\text{MeCO}_2)_2(4\text{-Phpy})_2(\text{H}_2\text{O})_{1.5}]$ (2). The same
80 reactions in absence of H₂O, using EtOH or MeOH as solvent, result in the formation of paddle-wheel
81 dimer $[\text{Cu}(\text{MeCO}_2)_2(4\text{-Phpy})_2]$ (3). Compound 2 can also be obtained via recrystallization of 3 in
82 MeOH:H₂O (1:1) mixture (Scheme 1). Therefore, the formation of a monomeric, 1 and 2, or a dimeric,
83 3, compound is controlled by the presence of a sizeable quantity H₂O in the reaction media (50%). Our
84 results agree with the fact that the role of water as one of the key factors governing the formation of
85 either monomeric or dimeric compounds has been already identified in the literature [7–11,13,18].
86 Furthermore, the use of different alcohols as co-solvents also results in the isolation of two differentiate
87 compounds, 1 in MeOH and 2 in EtOH.
88

89 Dimer 3 has already been described in the literature [17] but herein we report a different synthetic
90 procedure. In the reported procedure, the dimer was obtained working in a 1:1 metal to 4-Phpy ratio,
91 using a MeCN:MeOH:H₂O mixture (1:1:1, MeCN = acetonitrile) as solvent and heating at 60 °C for 15
92 min. Despite the presence of H₂O as co-solvent in the reported synthesis, the dimeric compound (3) is
93 obtained. This fact is probably due the heating at 60 °C, as it will be demonstrated later in this work.
94 The elemental analyses of 1–3 are consistent with the proposed formulas. Phase purity of 1–3 was
95 confirmed via Powder X-ray diffraction (PXRD) (Figs. S1–S3). ATR-FTIR spectrum of 1 and 2 show
96 significant shifts in the $\nu(\text{C}=\text{O})$ and $\nu(\text{C}-\text{O})$ stretching with respect to the spectra of
97 $[\text{Cu}(\text{MeCO}_2)_2(\text{H}_2\text{O})_2]$ (Figs. S4–S5), hence confirming the different coordination mode of the Cu(II) to
98 the carboxylate groups of MeCO₂ ligands. However, for compound 3 no significant variations could be
99 found in $\nu(\text{C}=\text{O})$ and $\nu(\text{C}-\text{O})$ stretching (Fig. S6). For 1–3, the presence of $\nu(\text{C}-\text{C})_{\text{ar}}$ and
100 $\nu(\text{C}-\text{N})_{\text{ar}}$ bands confirm the coordination of 4-Phpy. Additionally, the coordination mode of the
101 carboxylate groups can be inferred from the difference between the asymmetric and symmetric
102 vibrations of the COO⁻ groups ($D = \nu(\text{COO})_{\text{asym}} - \nu(\text{COO})_{\text{sym}}$) [19]. The values of $D = 215 \text{ cm}^{-1}$ for 1
103 and $D = 213 \text{ cm}^{-1}$ for 2 show a monodentate mode whereas for compound 3 $D = 189 \text{ cm}^{-1}$ shows
104 bidentate bridging mode [19]. For compound 2, the value (D) is coherent with its elucidated X-ray
105 crystal structure.

106 As described in Section 4.5, heating blue monomeric compounds 1 or 2 at 50 °C during 32 h resulted in
107 the formation of the green dimer 3. This conversion processes were confirmed via PXRD (Fig. 1). This
108 monomeric to dimeric conversion has also been reported previously in the literature [7–10,13]. It is also
109 noteworthy that this transformation also happens at room temperature when monomeric species are
110 treated with EtOH.

111 2.2. Crystal and extended structure of complex 2

112 Suitable crystals for X-ray diffraction were obtained via recrystallization of compound 3 in an
113 EtOH:H₂O mixture in a 1:1 proportion. The X-ray crystallographic analyses reveal that the crystal
114 structure of compound 2 contains two crystallographic independent monomers [Cu(MeCO₂)₂(4-
115 Phpy)₂(H₂O)₂] (2A) and [Cu (MeCO₂)₂(4-Phpy)₂(H₂O)] (2B) in its unit cell (Fig. 2). In each
116 monomer, the copper cation is linked to two monodentate MeCO₂ and two 4-Phpy ligands. The main
117 difference between the two monomers is due to the number of coordinated H₂O molecules that in turn
118 depends on the different conformations assumed by the acetate anions. Monomer 2A presents an
119 asymmetric unit consisting of a Cu(II) atom in a special position (inversion center), one monodentate
120 MeCO₂ anion, one 4-Phpy, and one H₂O molecule. Each of the independent Cu(II) center is six-
121 coordinated, having a distorted octahedral geometry. Monomer 2B, on the other hand, contains only one
122 H₂O molecule, resulting in a slightly distorted square pyramidal geometry (*s* = 0.093) [20]. In the
123 asymmetric unit the Cu1B atom is located on a twofold axis passing through Cu1B–O3B.

124 Therefore, the difference between the numbers of H₂O determines the coordination geometry of each
125 metal center. Selected distances and angles are provided on Table 1. For 2A, the basal plane is formed
126 by trans-coordinated 4-Phpy (Cu1A–N1A 2.028 (3) Å) and trans-coordinated monodentate MeCO₂
127 (Cu1A–O1A 1.984(2) Å). The apical positions are occupied by two weakly bonding oxygen atoms from
128 H₂O molecules (Cu1A–O3A 2.381(3) Å). This longer distance with respect to the basal plane can be
129 attributed to the Jahn–Teller effect. The other O2A atom of the acetate lies at a large distance (Cu1A ⋮
130 ⋮ O2A 3.300 Å) and is therefore, uncoordinated. Bond angles are in the range 85.24(11)°–94.76(11)°.
131 For 2B, 4-Phpy and acetate ligands form the basal plane (Cu1B–N1B 2.023(3) Å and Cu1A–O1A
132 1.951(2) Å) and a H₂O ligand is in the apical position (Cu1B–O3B 2.222(4) Å). Once again, the
133 uncoordinated O2B atom of the acetate ligand lies at a long distance (Cu1B ⋮ ⋮ O2B 3.126 Å). Short
134 bond angles are in the range of 88.18(8)°–94.16(9)° and long ones in the range of 170.77(18)°–
135 176.36(16)°. All these distances and angles are in good agreement with related acetate-pyridine
136 compounds [21–28].

137 The presence of two crystallographic monomeric subunits generates an intriguing supramolecular
138 structure, in which the coordinated H₂O molecules play a key role. Each subunit interacts exclusively
139 with its symmetry related subunits to generate 1D supramolecular chains, and each include only 2A
140 subunits or 2B subunits (Fig. 3, up). Those chains grow in a parallel fashion in the *b* direction and are
141 stacked alternatively in the *a* direction, forming a layered structure. Cu ⋮ ⋮ Cu distance between units
142 in the same chain is 5.867 Å for both Cu1A ⋮ ⋮ Cu1A and Cu1B ⋮ ⋮ Cu1B. Interlayer Cu1A ⋮ ⋮
143 ⋮ Cu1B distance is 8.361 Å. A similar supramolecular structure is seen in the closely related compounds
144 {[Cu(2,4-bipy)₂(MeCO₂)₂(H₂O)₂] ⋮ [Cu(2,4-bipy)₂(MeCO₂)₂(H₂O)]} (2,4-bipy = 2,4-bipyridine)
145 [27] and {[Cu(stpy)₂(MeCO₂)₂(H₂O)₂] ⋮ [Cu(stpy)₂(MeCO₂)₂(H₂O)]} (stpy = trans-4-styrylpyridine)
146 [28]. These two compounds also contain two crystallographic independent monomeric subunits, one
147 having an octahedral geometry and the other having a square pyramidal one, which form independent

148 1D chain containing only either octahedral or square pyramidal subunits. Furthermore, intrachain and
149 interlayer Cu... Cu distances show similar values for the three compounds. Interestingly, for these
150 two combinations of acetate and pyridine derivative ligands no dimeric structures have been found in the
151 literature.

152 The study of each individual chain reveals that their H-bridging interactions are different. Each
153 monomer 2A has a symmetric quadruple H-bond, involving O1A from the acetate ligand (which is the
154 coordinating oxygen) and H3OB from the H2O molecule (O3A–H3OB 0.832 Å, O1A... O3A–
155 H3OB 2.849 Å, O1A... H3OB– O3A 2.050 Å, O1A... H3OB–O3A 160.92°). Each Monomer
156 2B forms an asymmetric double bond, involving O2B from the acetate ligand (note that this is the non-
157 coordinating oxygen) and H3OC from the H2O molecule (O3B–H3OC 0.830 Å, O2B... O3C–
158 H3OC 2.719 Å, O2B... H3OC–O3B 1.903 Å, O2B... H3OC–O3B 167.13°) (Fig. 3, down).
159

160 **3. CONCLUSIONS**

161

162 Direct reaction of Cu(II) acetate with 4-phenylpyridine (4-Phpy) at room temperature and alcohol (EtOH
163 or MeOH) and H₂O as solvent, allowed the preparation of monomeric and dimeric compounds. The
164 formation of the monomeric or dimeric compounds depends on the solvent. When this solvent is alcohol
165 (EtOH or MeOH), the formation of the paddle-wheel compound (3) is observed, however, when the
166 solvent is an alcohol:H₂O (1:1) mixture, the monomeric compounds (1, 2) are obtained. The formation
167 of compounds 1 and 2 depends on the alcohol used, MeOH and EtOH, respectively, as confirmed via
168 PXRD. The three compounds have been fully characterized, and for the compound 2 the crystal and
169 molecular structure was determined by X-ray diffraction. The crystal structure reveals the presence of
170 two independent monomers (2A, 2B). Monomers 2A and 2B differ in the number of H₂O molecules
171 coordinated to the metal, two in the former, and one in the second. In the crystal packing of this
172 compound, the coordinated H₂O molecules play a key role generating two different 1D chains.

173

174 4. EXPERIMENTAL

175

176 4.1. General details

177 Copper(II) acetate monohydrate ($\text{Cu}(\text{MeCO}_2)_2 \cdot \text{H}_2\text{O}$), 4-phenylpyridine (4-Phpy) reagents, methanol
178 (MeOH) and ethanol (EtOH) were purchased from Sigma–Aldrich and used without further purification.

179 All the reactions and manipulations were carried out in air. Elemental analysis (C, H, N) were carried
180 out by the staff of Chemical Analysis Service of the Universitat Autònoma de Barcelona on a Thermo
181 Scientific Flash 2000 CHNS analyses. IR spectra were recorded on a Tensor 27 (Bruker) spectrometer,
182 equipped with and attenuated total reflectance (ATR) accessory model MKII Golden Gate with diamond
183 window in the range 4000–600 cm^{-1} . PXRD patterns were measured with Siemens D5000 apparatus
184 using the Cu K α radiation of 0.15418 nm. Patterns were recorded from $2\theta = 5^\circ - 50^\circ$, with a step scan
185 of 0.02° counting for 1 s. at each step.

186

187 4.2. Synthesis of $[\text{Cu}(\text{MeCO}_2)_2(4\text{-Phpy})_2(\text{H}_2\text{O})_2]$ (MeCO₂ = acetate, 4-Phpy = 4-phenylpyridine) (1)

188 To a solution containing 4-phenylpyridine (155 mg, 1.00 mmol) in MeOH (20 mL), a green solution of
189 $\text{Cu}(\text{MeCO}_2)_2 \cdot \text{H}_2\text{O}$ (198 mg, 0.99 mmol) in H₂O (20 mL) was added. The resulting light blue solution
190 was left to evaporate at room temperature. When the solution volume was reduced to 20 mL, a blue
191 crystalline solid appeared; it was filtered, washed with MeOH:H₂O (10 mL) and dried in the air.

192 1. Yield: 0.316 g (60.45%) (respect to $\text{Cu}(\text{MeCO}_2)_2 \cdot \text{H}_2\text{O}$). Elemental Analyses: Calc. for
193 $\text{C}_{26}\text{H}_{28}\text{N}_2\text{O}_6\text{Cu}$ (528.06): C 59.14; H 5.34; N 5.31. Found C 59.08; H 5.23; N 5.12%. ATR-FTIR
194 (wavenumber, cm^{-1}): 3336(br) [m(O–H), (H₂O)], 1654(m), 1612(s) [mas(COO)], 1562(s) 1484(m),
195 1397(s), 1332(s) [ms(COO)], 1332(m), 1231(w), 1162(w), 1073(w), 1044(w), 1016(m) [m(CO)],
196 931(w), 833(m), 764(m), 727(w), 688(m), 666(m), 623(w).

197

198 4.3. Synthesis of $[\text{Cu}(\text{MeCO}_2)_2(4\text{-Phpy})_2(\text{H}_2\text{O})_{1.5}]$ (MeCO₂ = acetate, 4-Phpy = 4-phenylpyridine) 199 (2)

200 To a solution containing 4-phenylpyridine (155 mg, 1.00 mmol) in EtOH (20 mL), a green solution of
201 $\text{Cu}(\text{MeCO}_2)_2 \cdot \text{H}_2\text{O}$ (198 mg, 0.99 mmol) in H₂O (20 mL) was added. The resulting light blue solution
202 was left to evaporate at room temperature. When the solution volume was reduced to 20 mL, a blue
203 crystalline solid appeared; it was filtered, washed with EtOH:H₂O (10 mL) and dried in the air. Suitable
204 crystals of 2 for X-ray diffraction (XRD) single crystal elucidation were obtained via recrystallization of
205 3 in an EtOH:H₂O mixture.

206 2. Yield: 0.365 g (71.03%). Elemental Analyses: Calc. for $\text{C}_{52}\text{H}_{54}\text{N}_4\text{O}_{11}\text{Cu}_2$ (1038.07): C, 60.16; H,
207 5.24; N, 5.40. Found C 60.24; H 5.07; N 5.33%. ATR-FTIR (wavenumber, cm^{-1}): 3358(br) [m(OH),
208 (H₂O)], 1591 [mas(COO)], 1567(s), 1483(m), 1393(s) [ms(COO)], 1378(m), 1332(w), 1221(w),
209 1072(w), 1038(w), 1016(m) [m(CO)], 928(w), 832(m), 762(m), 729(w), 690(m), 665(m), 618(w).

210

211 4.4. Synthesis of $[\text{Cu}(\text{MeCO}_2)_2(4\text{-Phpy})]_2$ ($\text{MeCO}_2 = \text{acetate}$, $4\text{-Phpy} = 4\text{-phenylpyridine}$) (3)

212 To a solution containing 4-phenylpyridine (157 mg, 1.01 mmol) in EtOH (20 mL), a green solution of
213 $\text{Cu}(\text{MeCO}_2)_2 \cdot \text{H}_2\text{O}$ (200 mg, 1.00 mmol) in EtOH (20 mL) was added. The resulting green solution
214 was allowed to evaporate at room temperature. When the solution volume was reduced to 20 mL, a
215 green crystalline solid appeared; it was filtered, washed with EtOH (5 mL) and dried in the air.

216 3. Yield: 0.313 g (92.93%) (respect to $\text{Cu}(\text{MeCO}_2)_2 \cdot \text{H}_2\text{O}$). Elemental Analyses: Calc. for
217 $\text{C}_{30}\text{H}_{30}\text{N}_2\text{O}_8\text{Cu}_2$ (673.64): C 53.49; H 4.49; N 4.16. Found C 53.28; H 4.37; N 4.09%. ATR-FTIR
218 (wavenumber, cm^{-1}): 1606(s) [mas(COO)], 1547(w), 1488(m), 1417(s) [ms(COO)], 1344(m), 1225
219 (w) 1073(w), 1048(w), 1026(w), 1012(m) [m(CO)], 923(w), 837(m), 759(m), 730(w), 692(m), 679(m),
220 619(w).

221 The same reaction has been assayed in MeOH resulting in the formation of the same compound with
222 similar yields.

223

224 4.5. Monomer–Dimer conversion

225 1 to 3: After heating a (107 mg, 0.20 mmols) of 1 for 32 h at 50 °C, the blue solid turned green. Yield:
226 0.049 g (71.7%).

227 2 to 3: Heating compound 2 (65 mg, 0.063 mmols) for 32 h. at 50 °C resulted in the formation of 3 in a
228 quantitative yield.

229 These conversion processes were confirmed via PXRD. These two transformations imply both
230 dehydration and sublimation of half of the coordinated 4-Phpy. In a separate experiment, we confirmed
231 that a sample of pure 4-Phpy in the same conditions sublimates completely.

232

233 4.6. X-ray crystal structure of 2

234 The X-ray intensity data for the crystallographic analysis were measured on a D8 Venture system
235 equipped with a multilayer mono-chromate and a Mo microfocus ($k = 0.71073 \text{ \AA}$) at 100 K. For the
236 compound $[\text{Cu}(\text{MeCO}_2)_2(4\text{-Phpy})_2(\text{H}_2\text{O})_2]$ [$\text{Cu}(\text{MeCO}_2)_2(4\text{-Phpy})_2(\text{H}_2\text{O})$] (2) a blue prism-like
237 specimen was used. The frames were integrated with the Bruker SAINT Software package using a
238 narrow-frame algorithm. Data were corrected for absorption effects using the multi-scan method
239 (SADABS). The calculated minimum and maximum transmission coefficients (based on crystal size) are
240 0.6580 and 0.7454.

241 The structure was solved using the Bruker SHELXTL Software, package and refined using SHELX
242 [29]. The final cell constants and volume, are based upon the refinement of the XYZ-centroids of
243 reflections above 20 $\sigma(I)$. Crystal data and relevant details of structure refinement are reported in Table
244 2. Complete information about the crystal structure and molecular geometry is available in CIF format
245 as Supporting Information. Molecular graphics were generated Mercury 3.6 software [30,31]. Color
246 codes for all molecular graphics: orange (Cu), blue (N), red (O), gray (C), White (H).

247

248 **ACKNOWLEDGEMENTS**

249

250 This work was financed by the Spanish National Plan of Research MAT2015-65756-R and by
251 2014SGR260 and 2014SGR377 projects from the Generalitat de Catalunya. J. S. also acknowledges the
252 Universitat Autònoma de Barcelona for his pre-doctoral grant.

253

254 **REFERENCES**

255

- 256 [1] J.M. Lehn, *Chem. Soc. Rev.* 46 (2017) 2378.
- 257 [2] N.N. Adarsh, P. Dastidar, *Chem. Soc. Rev.* 41 (2012) 3039.
- 258 [3] R. Chakrabarty, P.S. Mukherjee, P.J. Stang, *Chem. Rev.* 111 (2011) 6810.
- 259 [4] M. Alasaar, C. Tshcierske, M. Prehm, *Liq. Cryst.* 38 (2011) 925.
- 260 [5] M. Eddaoudi, J. Kim, D. Vodak, A. Sudik, J. Wachter, M. O’Keeffe, O.M. Yaghi, *PNAS* 99
261 (2002) 4900.
- 262 [6] G. Wang, Z. Xue, J. Pan, L. Wei, S. Han, J. Qian, Z. Wang, *CrystEngComm* 18 (2016) 8362.
- 263 [7] P. Sharrock, M. Melnik, *Can. J. Chem.* 63 (1985) 52.
- 264 [8] I.Y. Ahmed, A.L. Abu-Hijleh, *Inorg. Chim. Acta* 61 (1982) 241.
- 265 [9] A.L. Abu-Hijleh, *Polyhedron* 23 (1989) 2777.
- 266 [10] I. Uruska, J. Zielkewicz, *J. Sol. Chem.* 16 (1987) 145.
- 267 [11] F. Hamza, G. Kikcelbick, *Macromolecules* 42 (2009) 7762.
- 268 [12] B. Kozlevcar, A. Murn, K. Podlipnik, N. Lah, I. Leban, P. Segedin, *Croat. Chem. Acta* 77 (
269 2004) 613.
- 270 [13] C.-H. Ge, X.-D. Zhang, W. Guan, Q.-T. Liu, *J. Chem. Crystallogr.* 36 (2006) 459.
- 271 [14] J. Soldevila-Sanmartín, J.A. Ayllón, T. Calvet, M. Font-Bardia, J. Pons, *Inorg. Chem. Commun.*
272 71 (2016) 90.
- 273 [15] M. Guerrero, S. Vázquez, J.A. Ayllón, T. Calvet, M. Font-Bardia, J. Pons, *ChemSelect* 2 (2017)
274 632.
- 275 [16] J. Soldevila-Sanmartín, J.A. Ayllón, T. Calvet, M. Font-Bardia, J. Pons, *Polyhedron* 126 (2016)
276 184.
- 277 [17] M.-L. Tong, W. Lei, X.M. Chen, S.L. Zheng, S. Weng Ng, *Acta Cryst.* C58 (2002) m232.
- 278 [18] R.E. Del Sesto, A.M. Arif, J.S. Miller, *Inorg. Chem.* 39 (2009) 4894.
- 279 [19] K. Nakamoto, *Infrared and Raman Spectra of Inorganic and Coordination Compounds.*
280 *Applications in Coordination, Organometallic and Bioinorganic Chemistry*, sixth ed. Wiley-
281 Interscience, New York, USA, 2009.
- 282 [20] A.W. Addison, T.N. Rao, *J. Chem. Soc., Dalton Trans.* 7 (1984) 1349.
- 283 [21] L. Sieron, *Acta Cryst.* E63 (2007) m1659.
- 284 [22] C.H. Ge, X.D. Zhang, W. Guan, Q.T. Liu, *J. Chem. Crystallogr.* 36 (2006) 459.
- 285 [23] J. Moncol, M. Mudra, P. Lönnecke, M. Hewitt, M. Valko, H. Morris, J. Svorec, M. Melnik, M.
286 Mazur, M. Koman, *Inorg. Chim. Acta* 360 (2007) 3213.
- 287 [24] M. Puchonova, Z. Repicka, J. Moncol, Z. Ruzikova, M. Mazur, *J. Molec. Structr.* 1092 (2015) 1.
- 288 [25] M. Du, X.H. Bu, Y.M. Guo, H. Liu, *Inorg. Chem.* 41 (2002) 4904.
- 289 [26] Y.X. Zhou, X. Li, H.Y. Zhang, C.L. Fang, H.Y. Zhang, B.L. Wu, *J. Coord. Chem.* 64 (2011)
290 4066.

- 291 [27] R. Kryszynski, A. Adamczyk, J. Radwanska-Doczekalska, T. Bartczak, J. Coord. Chem. 55
292 (2002) 1209.
- 293 [28] C. Karunakaran, K.R.J. Thomas, A. Shunmugasunadaran, R. Murugesan, J. Chem. Crystalslogr.
294 30 (2000) 351.
- 295 [29] G.M. Sheldrick, Acta Cryst. C71 (2015) 3.
- 296 [30] C.F. Macrae, P.R. Edgington, P. McCabe, E. Pidcock, G.P. Shields, R. Taylor, M. Towler, J.
297 van de Streek, J. Appl. Crystallogr. 39 (2006) 453.
- 298 [31] C.F. Macrae, I.J. Bruno, J.A. Chisholm, P.R. Edgington, P. McCabe, E. Pidcock, L. Rodriguez-
299 Monge, R. Taylor, J. van de Streek, P.A. Wood, J. Appl. Crystallogr. 41 (2008) 466.
- 300

301 **Legends to figures**

302

303 **Figure. 1** PXRD patterns of 1 (top), 2 (middle) and 3 (bottom).

304

305 **Figure. 2** Monomers 2A and 2B, and their corresponding numbering scheme for relevant atoms.

306 Hydrogens are omitted for the sake of clarity.

307

308 **Figure. 3** View of the stacking of Monomers 2A and 2B along the a axis (up). Detailed view of the H-

309 bonding interactions in the individual chains (down).

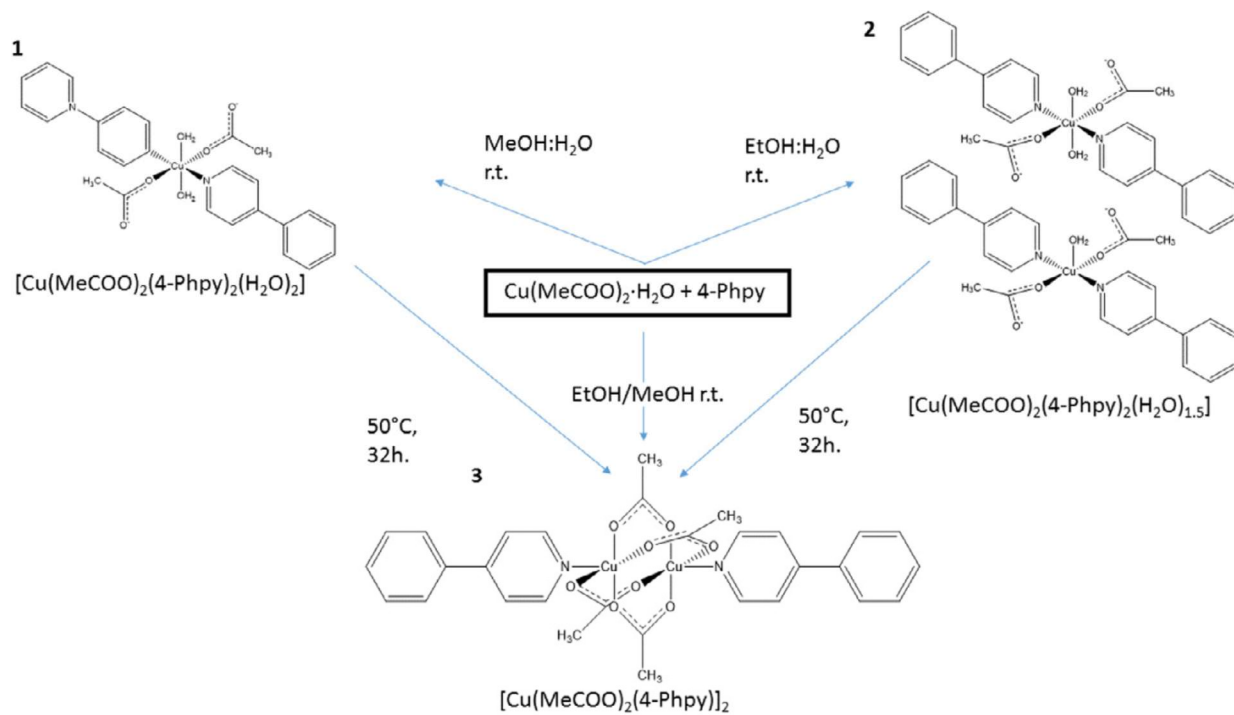
310

311

312

SCHEME 1

313

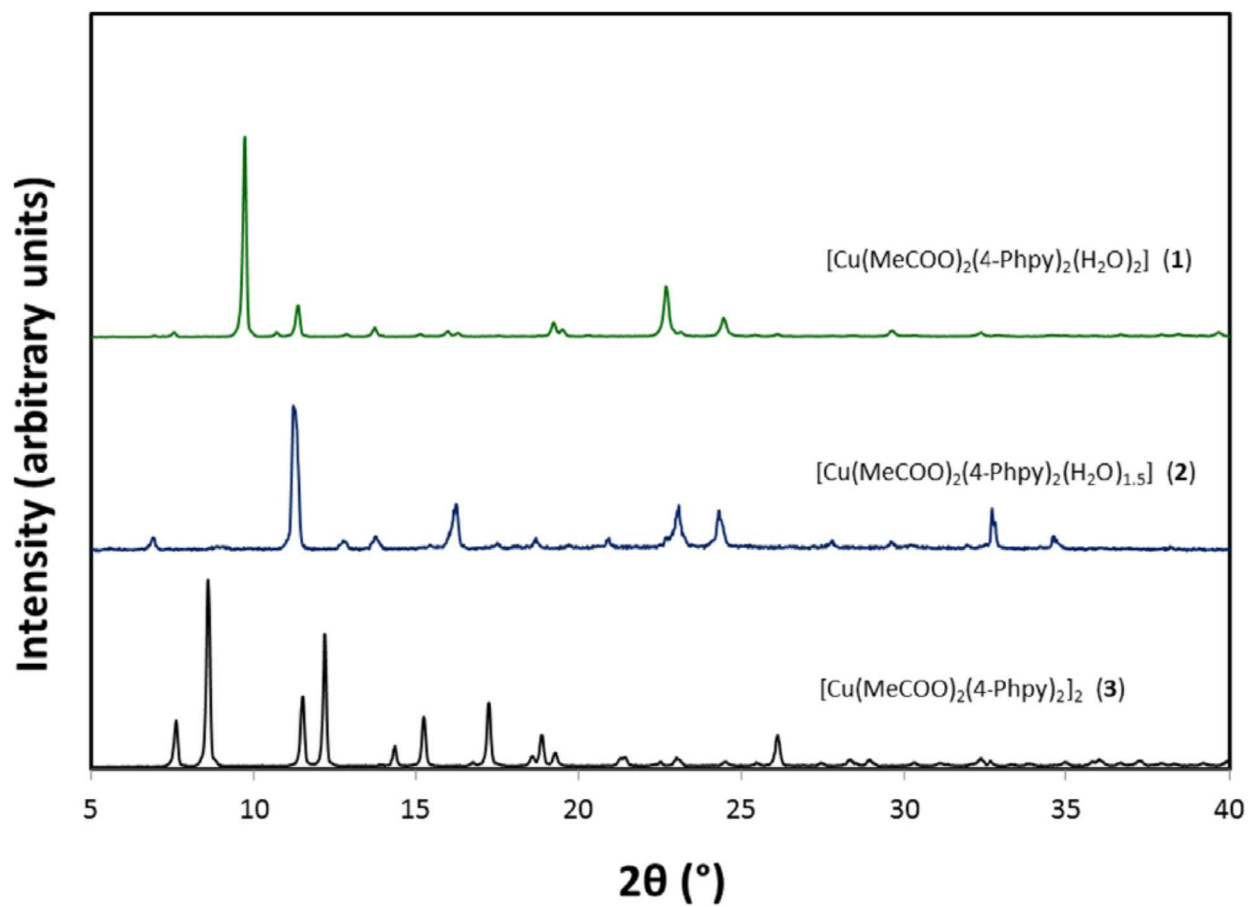


314

315

FIGURE 1

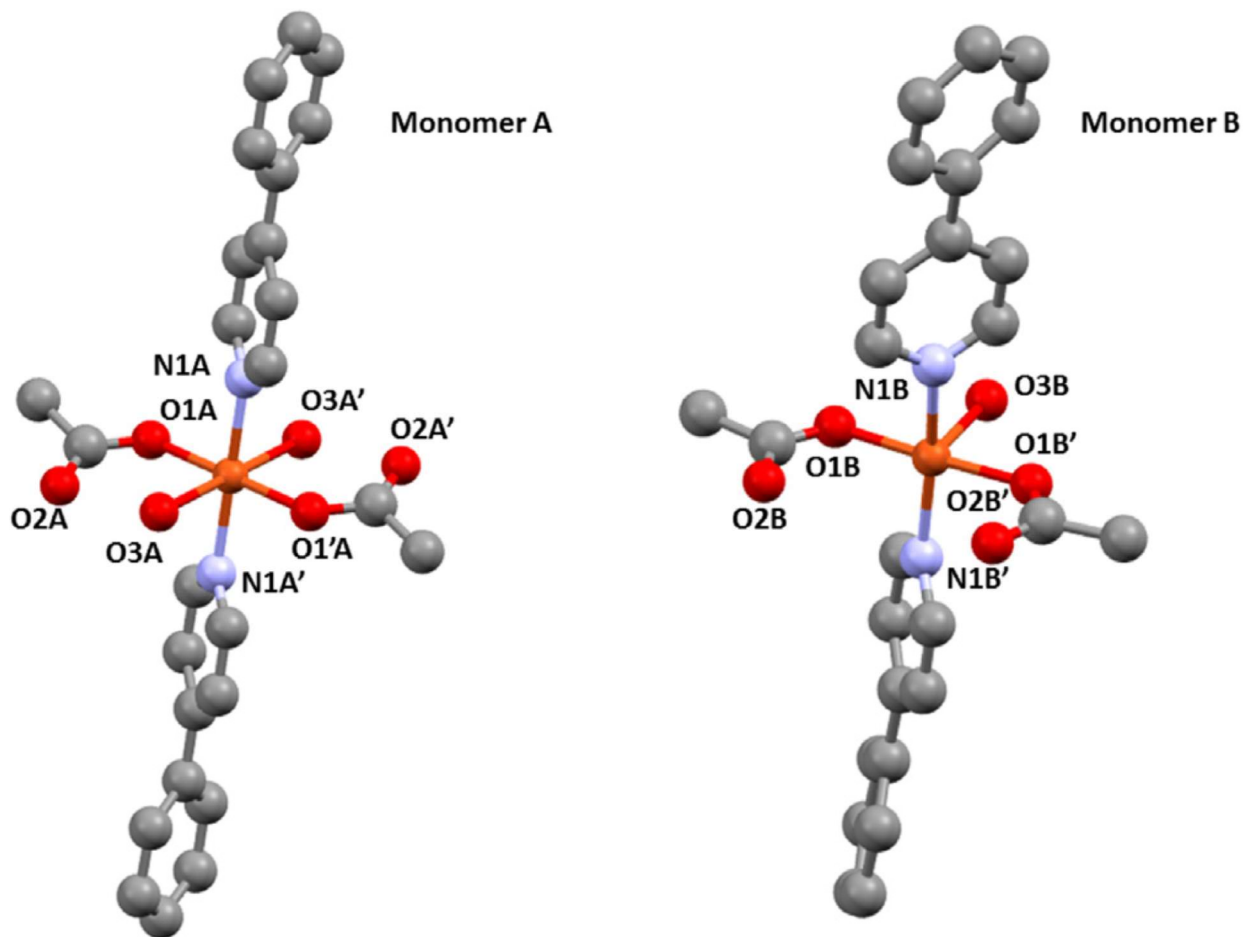
316
317
318



319
320
321

322
323
324
325
326

FIGURE 2



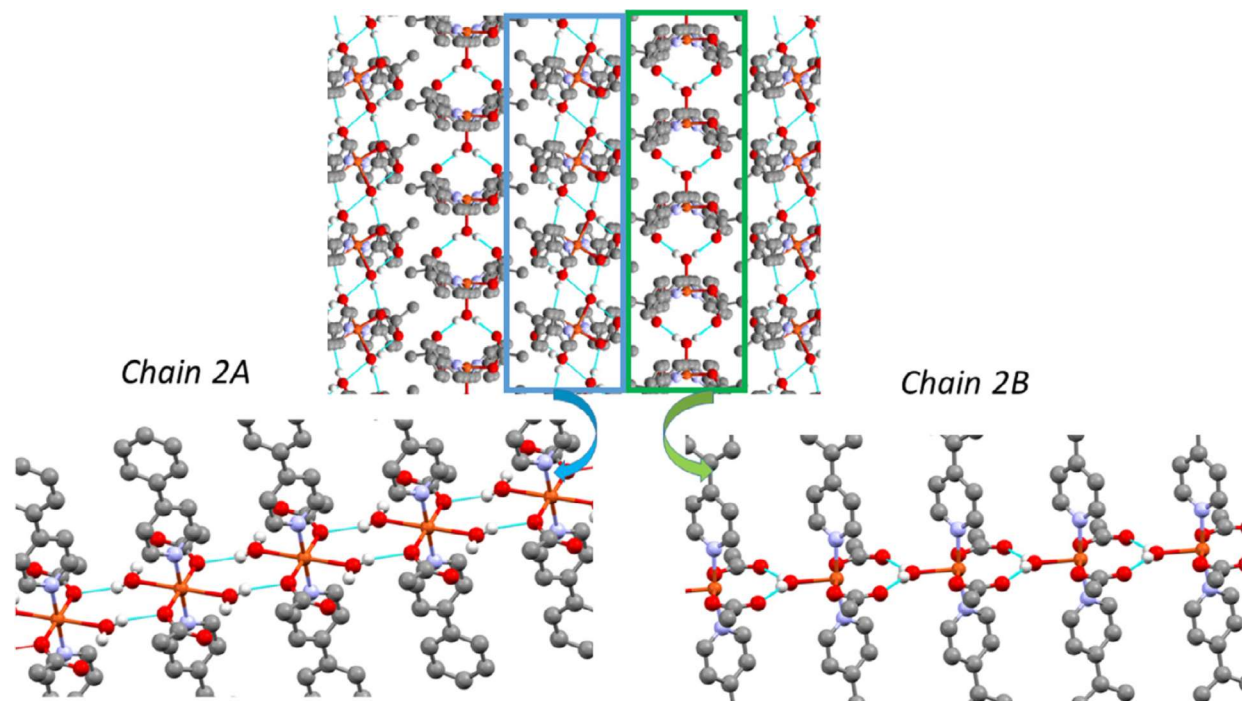
327
328

329

FIGURE 3

330

331



332

333

334
 335
 336
 337
 338

Table 1 Selected bond lengths (Å) and bond angles (°) values for (2A) and (2B). The estimated standard deviations (e.s.d.s.) are shown in parentheses.

Molecule A			
<i>Bond lengths (Å)</i>			
Cu(1A)–O(1A)	1.984(2)	Cu(1A)–O(3A)	2.381(3)
Cu(1)–N(1A)	2.028(3)		
<i>Bond angles (°)</i>			
O(1A)–Cu(1A)–O(1A)#1	180.0	N(1A)–Cu(1)–O(3A)#1	85.24(11)
O(1A)–Cu(1A)–N(1A)#1	88.11(11)	O(1A)–Cu(1A)–O(3A)	86.80(10)
O(1A)–Cu(1A)–N(1A)	91.89(11)	N(1A)–Cu(1A)–O(3A)	94.76(11)
N(1A)#1–Cu(1A)–N(1A)	180.0	O(3A)#1–Cu(1A)–O(3A)	180.0
O(1A)–Cu(1A)–O(3A)#1	93.20(10)		
Molecule B			
<i>Bond lengths (Å)</i>			
Cu(1B)–O(1B)	1.951(2)	Cu(1B)–O(3B)	2.222(4)
Cu(1B)–N(1B)	2.023(3)		
<i>Bond angles (°)</i>			
O(1B)–Cu(1B)–O(1B)#2	176.36(16)	N(1B)#2–Cu(1B)–N(1B)	170.77(18)
O(1B)–Cu(1B)–N(1B)#2	89.34(11)	O(1B)–Cu(1B)–O(3B)	88.18(8)
O(1B)–Cu(1B)–N(1B)	90.95(11)	N(1B)–Cu(1B)–O(3B)	94.61(9)
#1 = –x+1, –y, –z+1; #2 = –x+1, y, –z+1/2			

339
 340
 341
 342

343 **Table 2** Crystallographic data for [Cu(MeCO₂)₂(4-Phpy)₂(H₂O)₂] [Cu(MeCO₂)₂(4-Phpy)₂(H₂O)] (2).
 344

Formula	C ₃₂ H ₃₆ N ₄ O ₁₁ Cu ₂
Formula weight	1038.07
T (K)	100(2)
λ (Å)	0.71073
System, space group	monoclinic, C2/c
a (Å)	25.181(2)
b (Å)	5.8668(5)
c (Å)	30.879(3)
α (°)	90
β (°)	94.496(4)
γ (°)	90
U (Å ³)Z	4547.7(7)/4
D _{calc} (g cm ⁻³)/μ (mm ⁻¹)	1.516/1.005
F(000)	2160
Crystal size (mm ³)	0.279x0.075x0.063
hkl ranges	-31 ≤ h ≤ 31, -7 ≤ k ≤ 7, -38 ≤ l ≤ 38
2θ range (°)	2.173–26.440
Reflections collected/unique/[R _{int}]	38487/4682 [R _{int} = 0.0570]
Completeness to θ (%)	99.9
Absorption correction	semi-empirical
Maximum and minimum trans.	0.7454 and 0.6580
Data/restraints/parameters	4682/4/325
Goodness-of-fit (GOF) on F ²	1.279
Final R indices [I > 2σ(I)]	R ₁ = 0.0542, wR ₂ = 0.1200
R indices (all data)	R ₁ = 0.0605, wR ₂ = 0.1223
Extinction coefficient	n/a
Largest difference peak and hole (e Å ⁻³)	+0.709, -1.441

345